Electronic Supplementary Information

for

Catalytically Active Nanosized Pd_9Te_4 (Telluropalladinite) and Pdte (Kotulskite) Alloys: First Precursor-Architecture Controlled Synthesis using Organotellurium Compounds as Single Source Precursors

Aayushi Arora,[a] Preeti Oswal,[a] Gyandshwar K. Rao,[b] Sushil Kumar,[a] Ajai K. Singh,[c] Arun Kumar*[a]

[a]Department of Chemistry, School of Physical Sciences, Doon University, Dehradun, Uttarakhand, 248012 (India)

[b]Department of Chemistry, Amity School of Applied Sciences, Amity University Haryana (AUH), Gurgaon, Haryana, 122413 (India)

[c]Department of Chemistry, Indian Institute of Technology Delhi, New Delhi, 110016 (India)

Section 1. NMR and HRMS Spectra

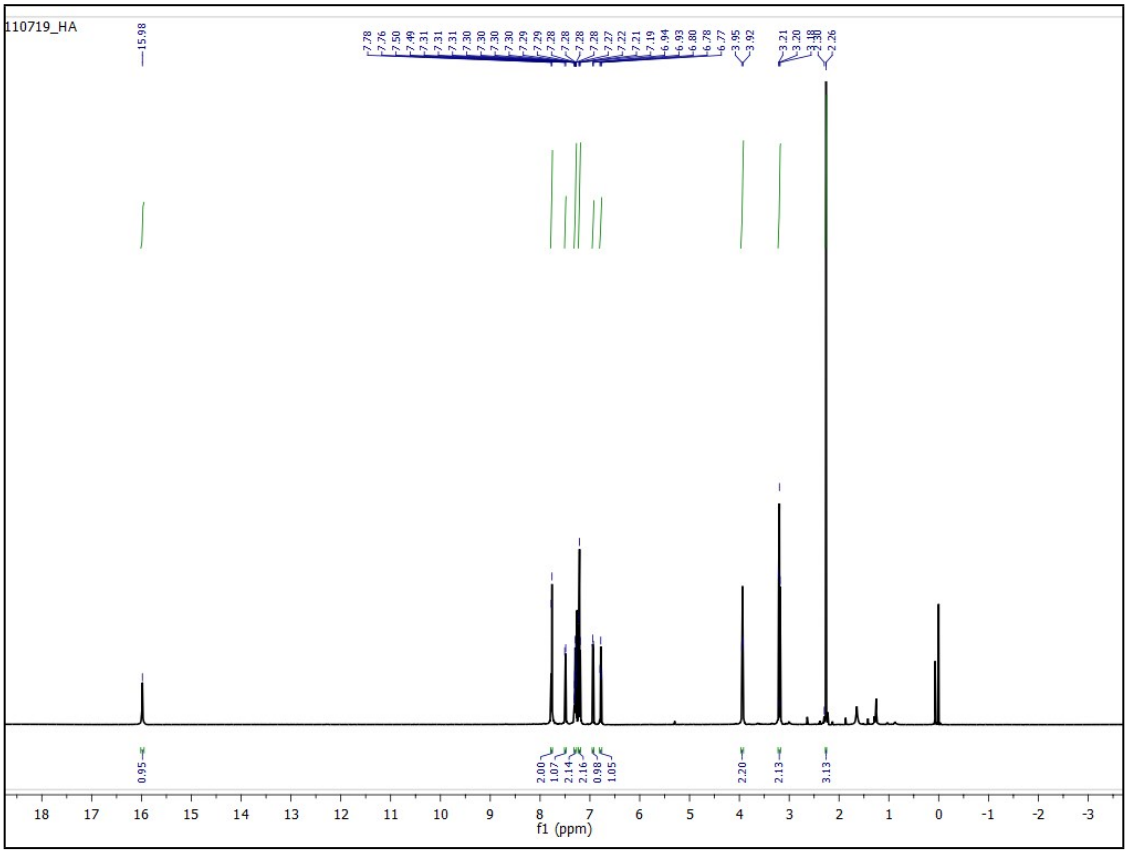

Figure S1. ^{1}H NMR of **L2**

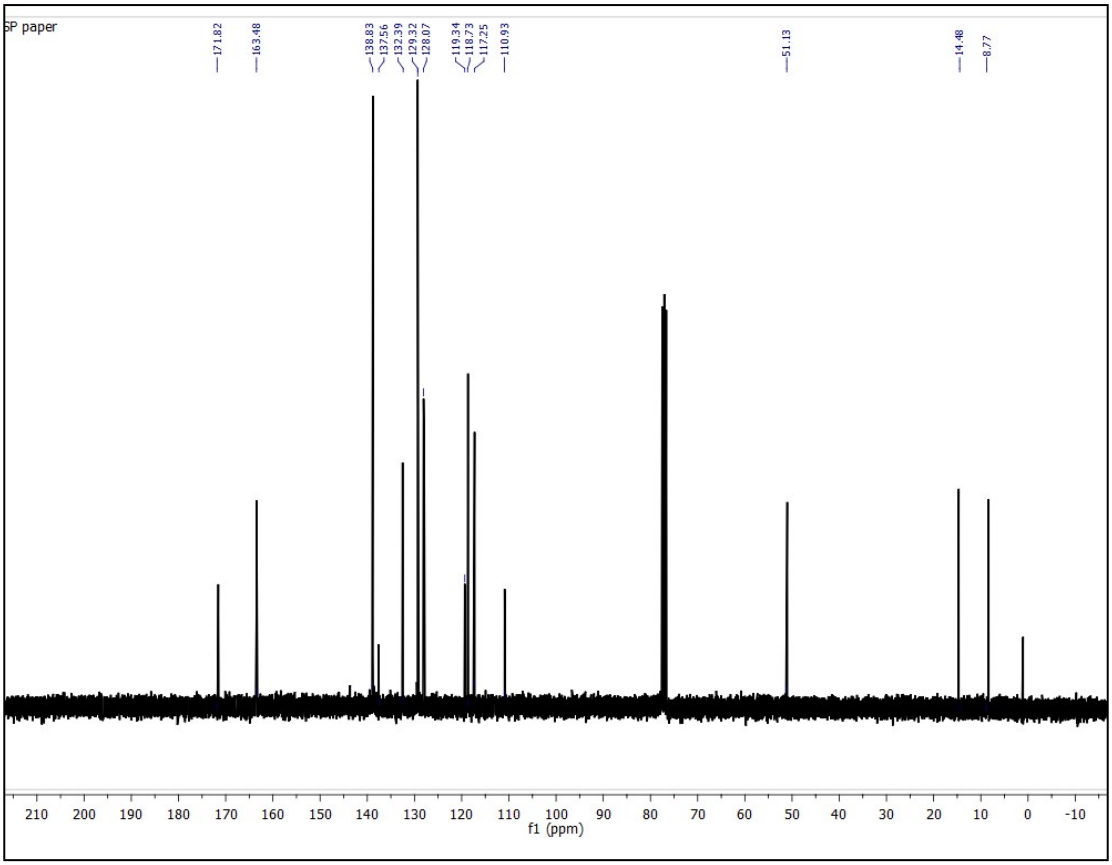

Figure S2. ^{13}C NMR of **L2**

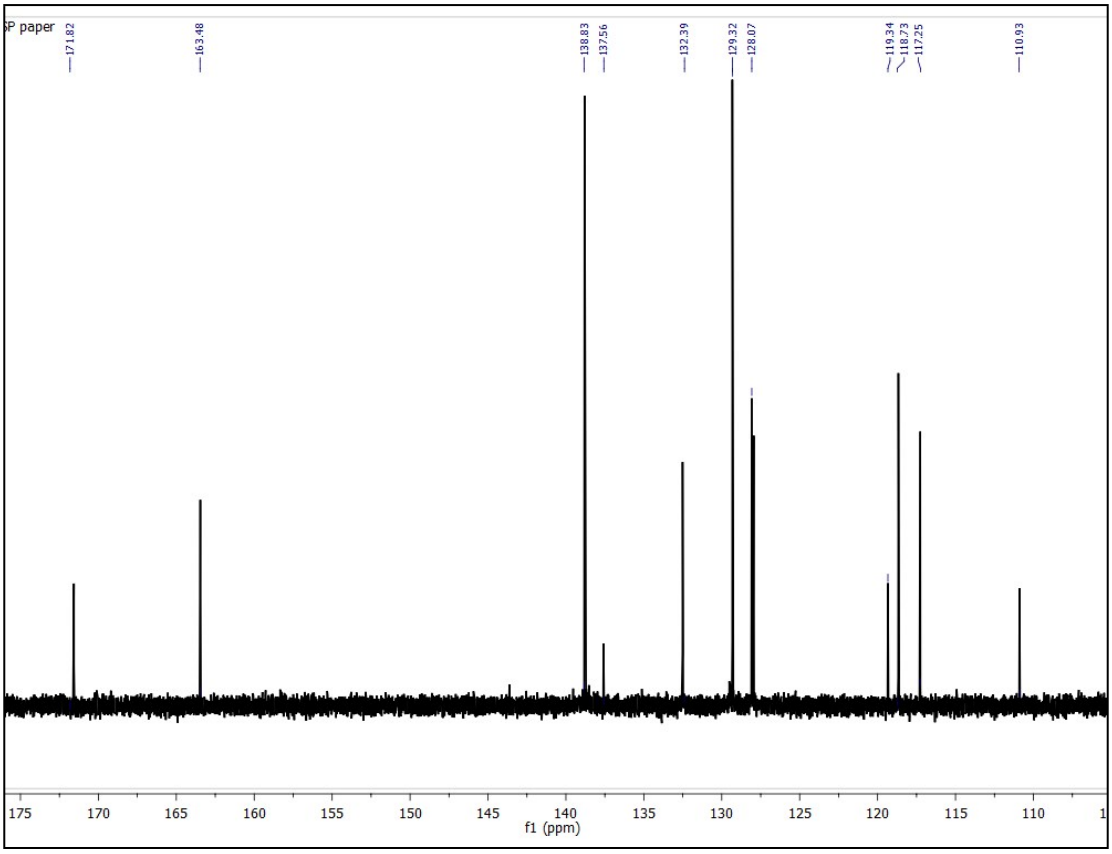

Figure S3. Magnified view of ^{13}C NMR of **L2**

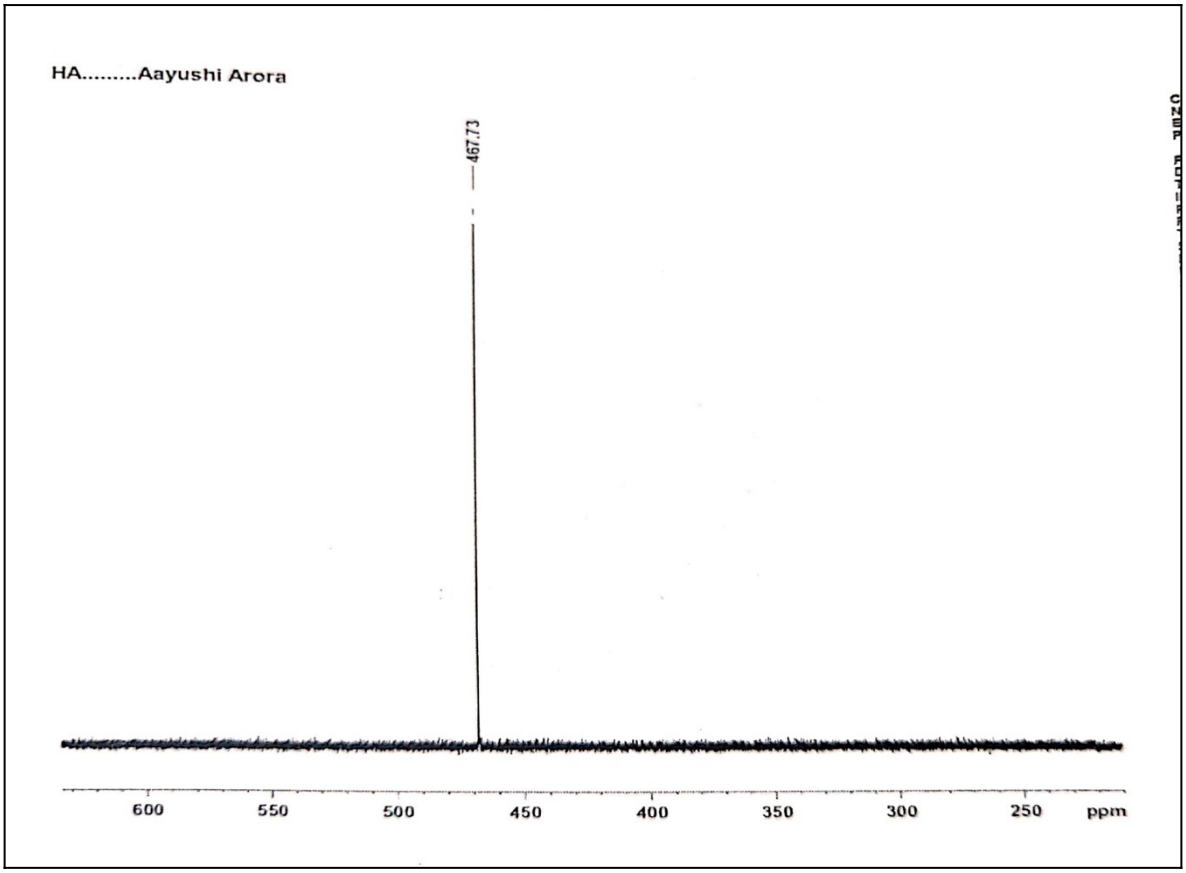

Figure S4. ^{125}Te NMR of **L2**

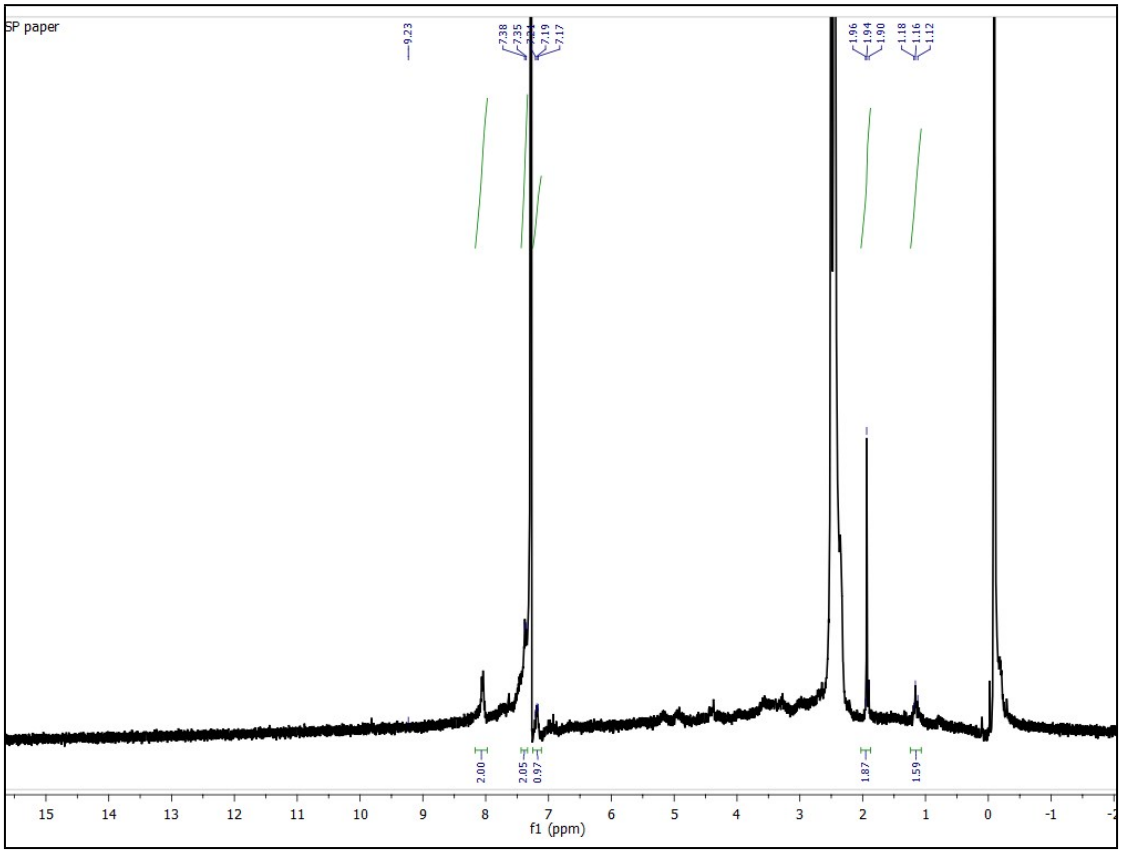

Figure S5. ^{1}H NMR of **1**

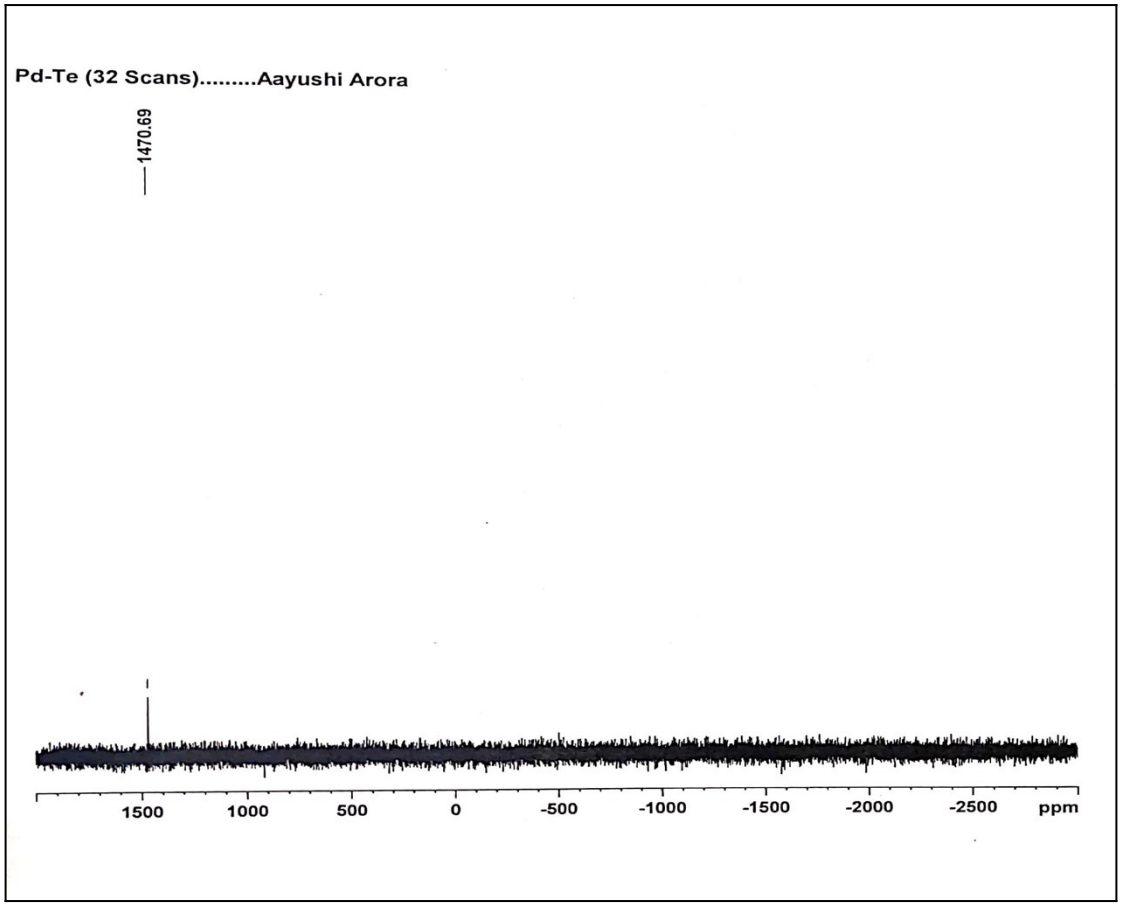

Figure S6. ^{125}Te NMR of **1**

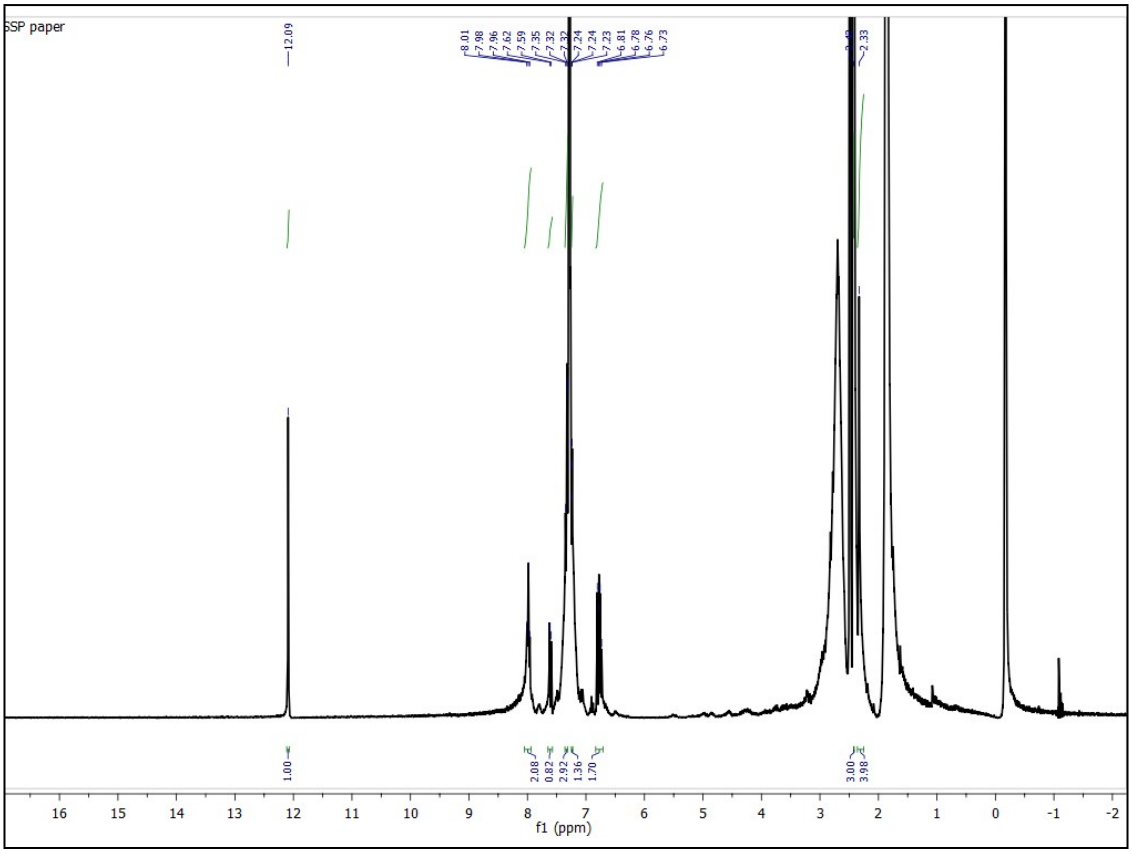

Figure S7. ^{1}H NMR of **2**

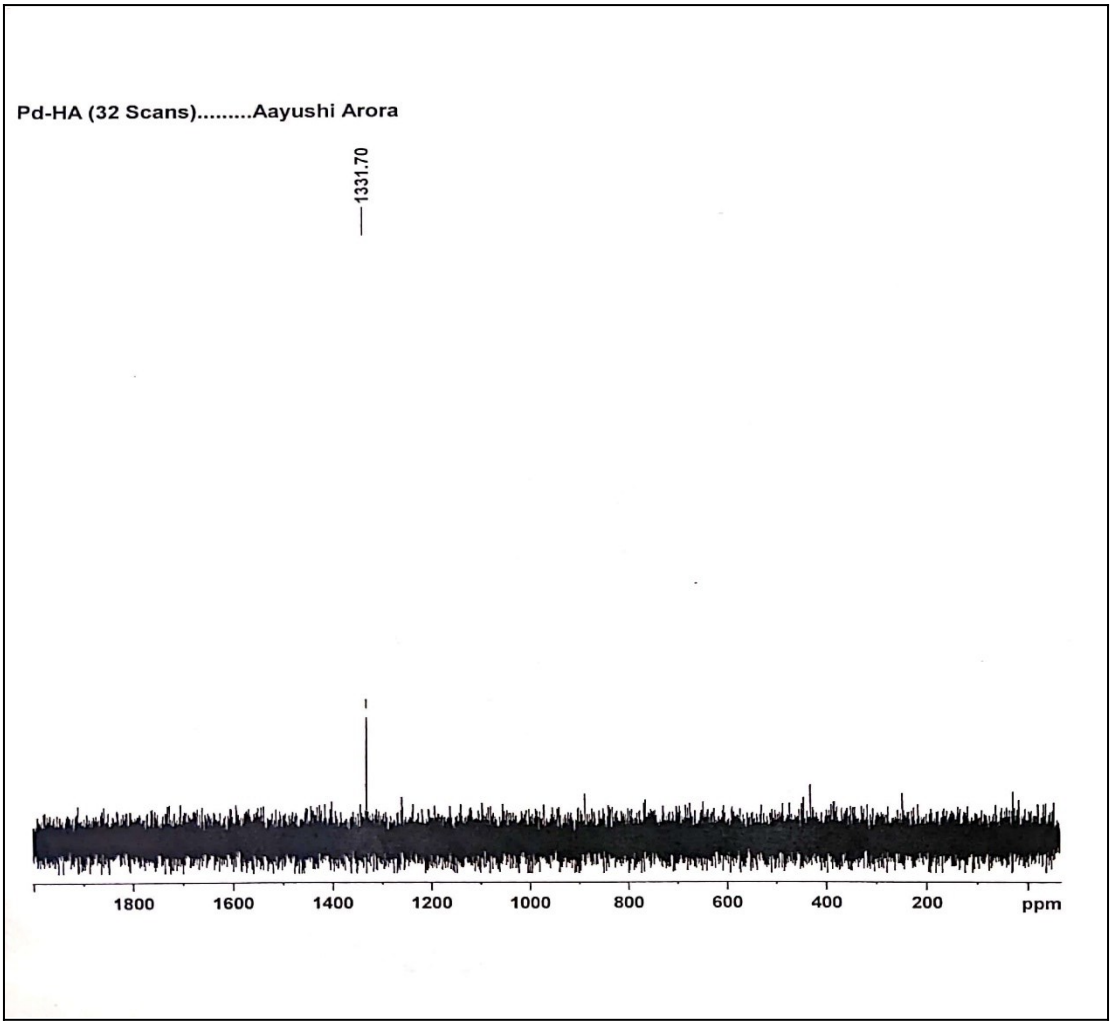

Figure S8. ^{125}Te NMR of **2**

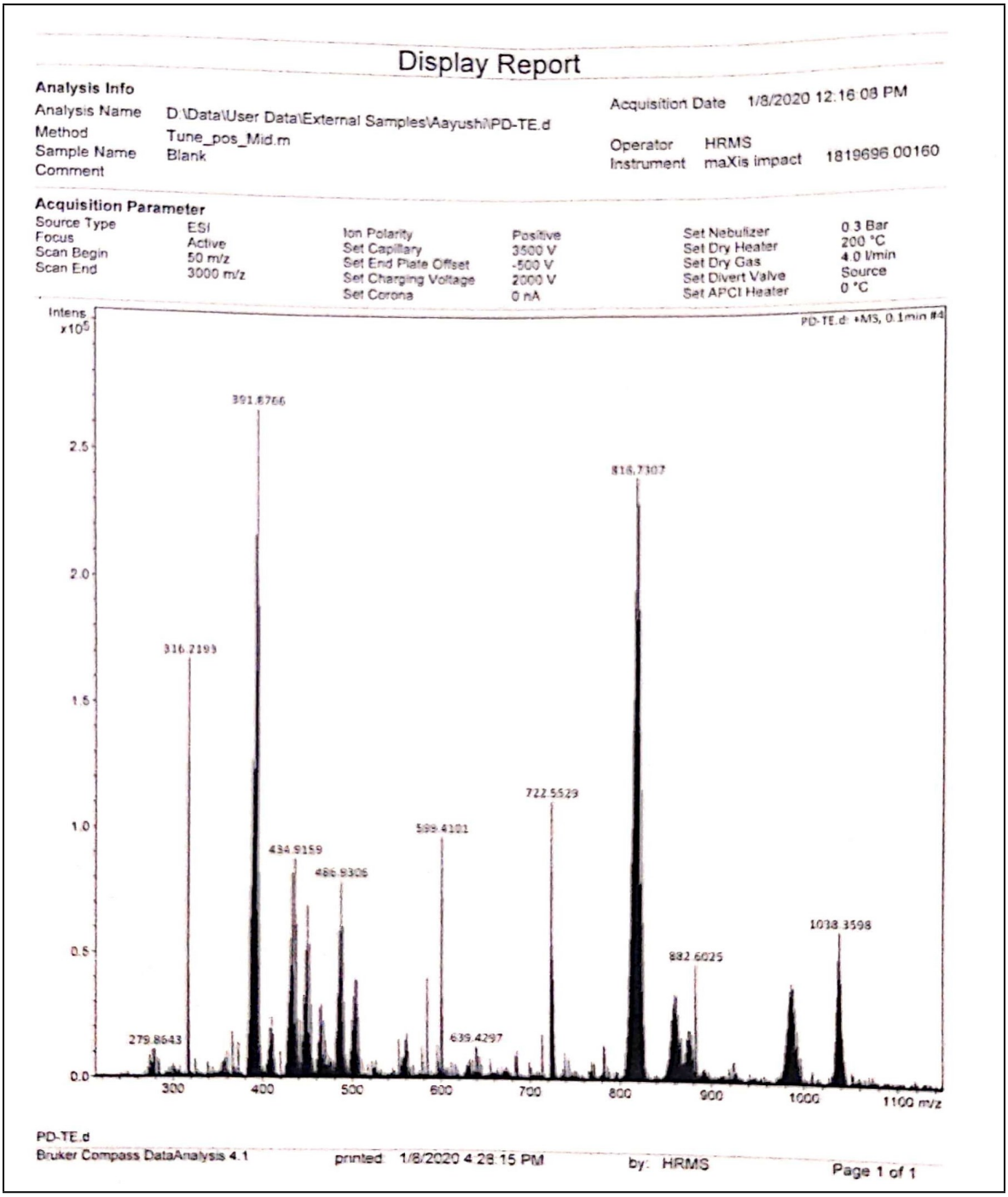

Figure S9. Mass spectra of **1**

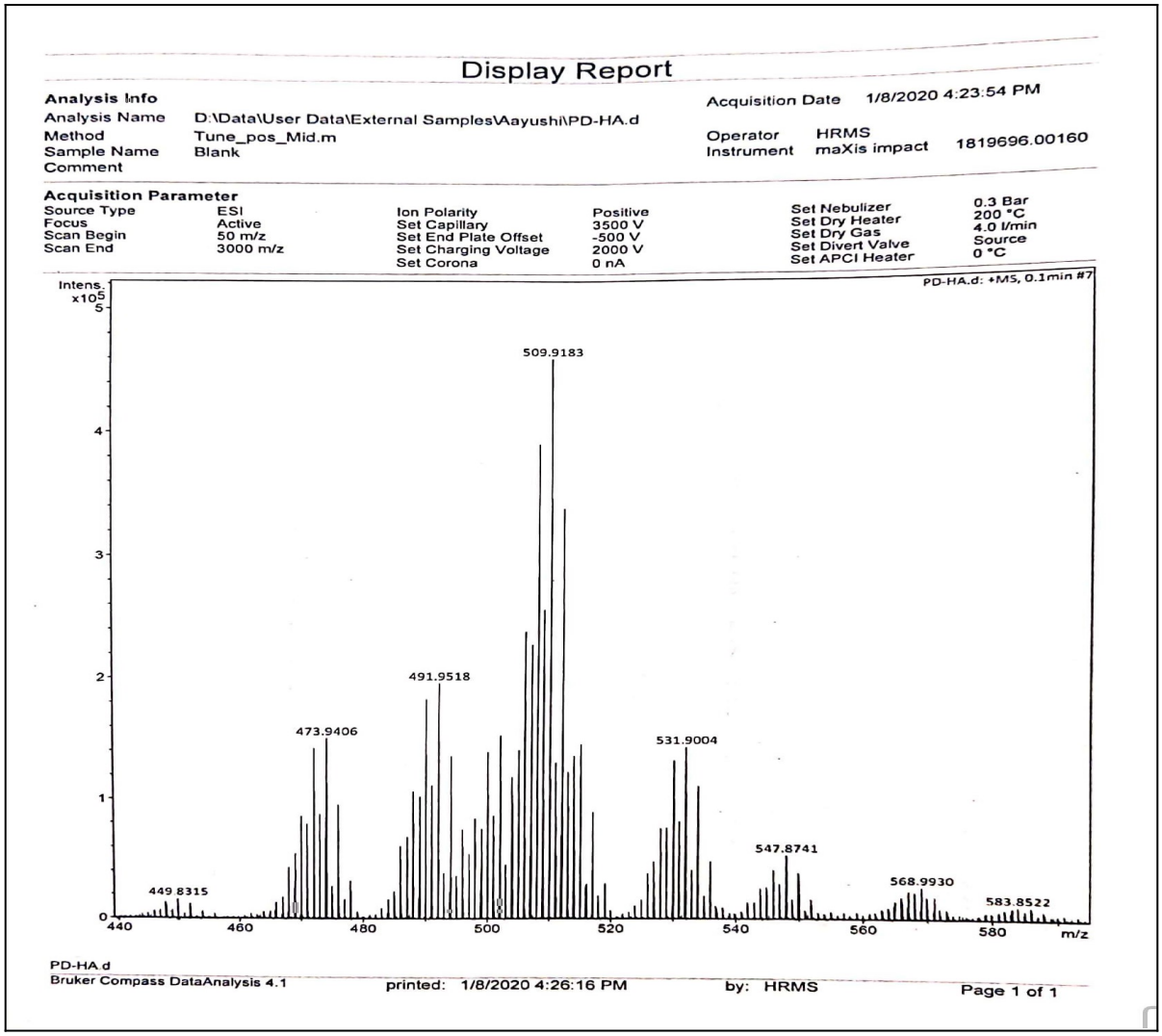

Figure S10. Mass spectra of **2**

Section 2: Structure Elucidation via Single Crystal X ray Diffraction

The crystal structures of both the palladium complexes depicting the assignment of all atoms are shown below in Figure S11 and S12. The details of all the bond parameters are summarized below in Table S2 and S3.

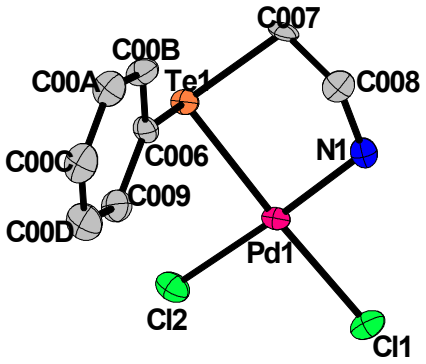

Figure S11. Crystal structure of **1**

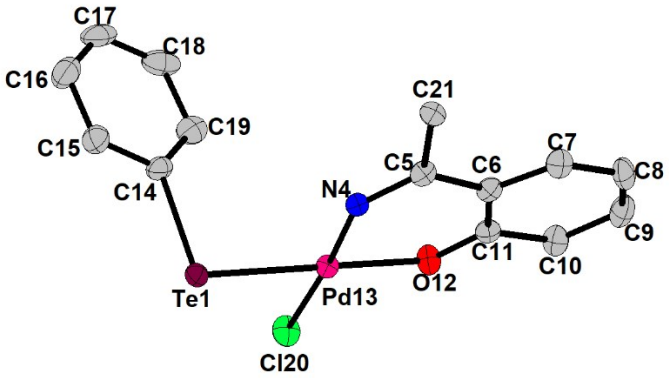

Figure S12. Crystal structure of **2**

Table S1. Bond angles and bond lengths of **1**

Bond Lengths (Å)		**Bond Angles (°)**	
C(006)−C(009)	1.399(8)	C(006)−Te(1)−Pd(1)	98.03(15)
C(006)−C(00B)	1.388(8)	C(006)−Te(1)−C(007)	94.5(2)
C(007)−C(008)	1.505(8)	C(007)−Te(1)−Pd(1)	89.64(15)
C(009)−C(00D)	1.403(9)	Cl(2)−Pd(1)−Te(1)	88.82(4)
C(00A)−C(00B)	1.390(8)	Cl(2)−Pd(1)−Cl(1)	94.42(6)
C(00A)−C(00C)	1.366(9)	Cl(1)−Pd(1)−Te(1)	176.71(4)
C(00C)−C(00D)	1.374(9)	N(1)−Pd(1)−Te(1)	88.21(13)
Te(1)−Pd(1)	2.5057(6	N(1)−Pd(1)−Cl(2)	177.02(13)
Te(1)−C(006)	2.118(6)	N(1)−Pd(1)−Cl(1)	88.54(14
Te(1)−C(007)	2.149(6)	C(008)−N(1)−Pd(1)	116.6(4)
Pd(1)−Cl(2)	2.3142(16)	C(009)−C(006)−Te(1)	119.4(5)
Pd(1)−Cl(1)	2.3710(15)	C(00B)−C(006)−Te(1)	121.6(4)
Pd(1)−N(1)	2.063(5)	C(00B)−C(006)−C(009)	118.8(6)
		C(008)−C(007)−Te(1)	106.9(4)
		N(1)−C(008)−C(007)	112.3(5)
		C(006)−C(009)−C(00D)	119.2(6)
		C(00C)−C(00A)−C(00B)	120.0(6)
		C(006)−C(00B)−C(00A)	121.0(6)
		C(00A)−C(00C)−C(00D)	120.2(6)
		C(00C)−C(00D)−C(009)	120.7(6)

Table S2. Bond angles and bond lengths of **2**

Bond Lengths (Å)		**Bond Angles (°)**	
Te(1)−Pd(13)	2.5002(4)	C(2)−Te(1)−Pd(13)	87.59(12)
Te(1)−C(2)	2.120(4)	C(14)−Te(1)−Pd(13)	98.19(13)
Te(1)−C(14)	2.123(5)	C(14)−Te(1)−C(2)	95.38(17)
Pd(13)−Cl(20)	2.3271(11)	Cl(20)−Pd(13)−Te(1)	86.74(3)
Pd(13)−O(12)	2.007(3)	Cl(20)−Pd(13)−Pd(23)	96.02(3)
Pd(13)−N(4)	2.017(4)	O(12)−Pd(13)−Te(1)	175.15(9)
O(12)−C(11)	1.306(5)	O(12)−Pd(13)−Cl(20)	88.98(9)
N(4)−C(5)	1.319(5)	N(4)−Pd(13)−Te(1)	90.94(10)
N(4)−C(3)	1.485(3)	N(4)−Pd(13)−Cl(20)	175.89(11)
C(11)−C(6)	1.428(6)	N(4)−Pd(13)−O(12)	93.18(13)
C(11)−C(10)	1.415(6)	C(11)−O(12)−Pd(13)	125.8(3)
C(5)−C(6)	1.473(6)	C(5)−N(4)−Pd(13)	124.4(3)
C(5)−C(21)	1.528(6)	C(3)−N(4)−Pd(13)	118.7(3)
C(2)−C(3)	1.517(6)	C(3)−N(4)−C(5)	116.2(4)
C(6)−C(7)	1.408(6)	C(6)−C(11)−O(12)	125.8(4)
C(14)−C(19)	1.380(7)	C(10)−C(11)−O(12)	116.0(4)
C(14)−C(15)	1.397(6)	C(10)−C(11)−C(6)	118.2(4)
C(10)−C(9)	1.380(7)	C(6)−C(5)−N(4)	125.3(4)
C(7)−C(8)	1.367(6)	C(21)−C(5)−N(4)	118.7(4)
C(8)−C(9)	1.393(7)	C(21)−C(5)−C(6)	115.9(4)
C(18)−C(17)	1.368(8)	C(2)−C(3)−N(4)	113.8(4)
C(17)−C(16)	1.366(8)	C(5)−C(6)−C(11)	123.9(4)
		C(7)−C(6)−C(11)	117.2(4)
		C(7)−C(6)−C(5)	118.9(4)
		C(19)−C(14)−Te(1)	122.4(4)
		C(15)−C(14)−Te(1)	117.6(4)
		C(15)−C(14)−C(19)	119.8(5)
		C(9)−C(10)−C(11)	122.4(4)
		C(9)−C(10)−H(10)	118.8(3)
		C(8)−C(7)−C(6)	123.4(4)
		C(9)−C(8)−C(7)	119.6(4)
		C(8)−C(9)−C(10)	119.1(4)
		C(18)−C(19)−C(14)	119.8(5)
		C(16)−C(15)−C(14)	119.4(5)
		C(17)−C(18)−C(19)	119.9(5)

		C(16)−C(17)−C(18)	120.8(5)

Section 3: X-Ray Photoelectron Spectroscopy

The full binding energy region and Te−3d region are depicted in high resolution XPS spectra (Figure S13 and S14). The different values obtained for binding energy in both the cases are summarised in Table S3. The values for both Pd−3d and Te−3d agree with the previous literature [1,2].

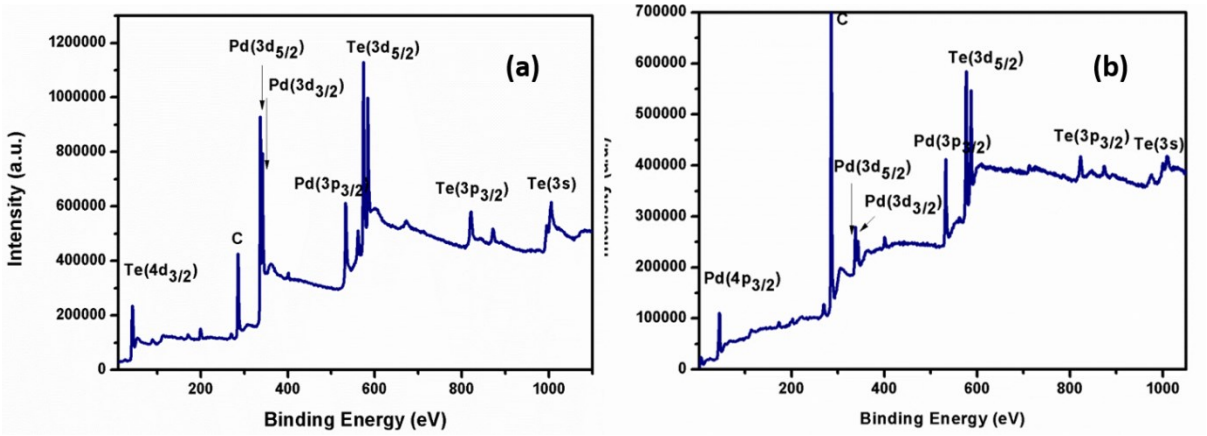

Figure S13. XPS spectra of Pd_9Te_4 (a) and PdTe (b) nanostructures

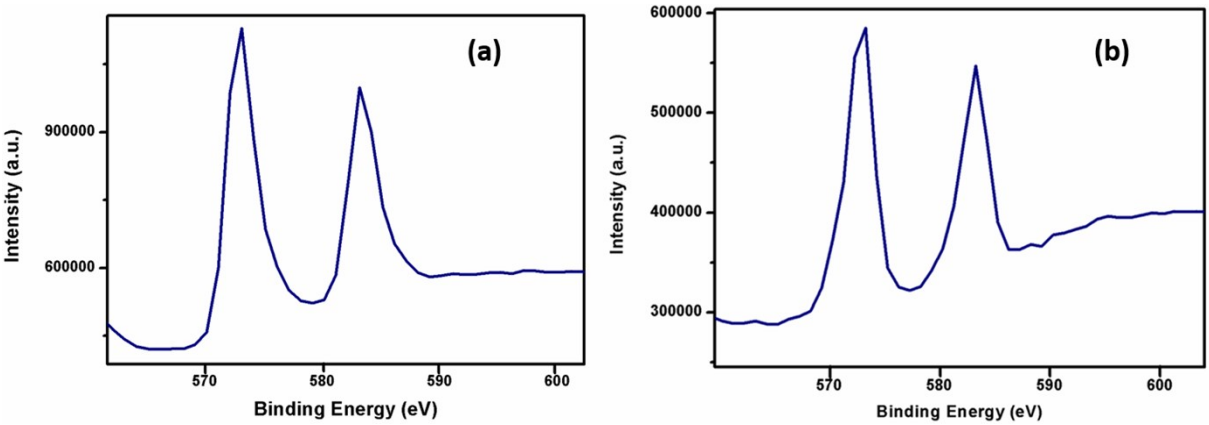

Figure S14. Tellurium 3d spectra of Pd_9Te_4 (a) and PdTe (b) nanostructures

Table S3. (a) Binding energy values of Pd-3d peak and (b) Te-3d peak in different phases

(a)

Material	Peak position (lower region)	Peak position (higher region)
Pd_9Te_4	336.08	341.39
	337.12	342.08
PdTe	337.80	343.08

Material	Peak position (lower region)	Peak position (higher region)

(b)

Pd_9Te_4	573.60	582.50
PdTe	574.29	583.10

Table S4. Optimization of reaction conditions for Suzuki Miyaura C-C coupling reaction

Entry No.	**Solvent**	**Base**	**Yield (%)**
1	DMF : Water (4:1)	Cs_2CO_3	43
2	DMF : Water (4:1)	K_2CO_3	88
3	DMF : Water (4:1)	CH_3COONa	No Conversion
4	DMF : Water (4:1)	NaOH	No Conversion
5	DMF	K_2CO_3	87
6	Toluene	K_2CO_3	65
7	THF	K_2CO_3	15
8	EtOH : Water (9:1)	K_2CO_3	17

Reaction Conditions: 4-Chlorobenzaldehyde (1.0 mmol), Phenyl boronic acid (1.1 mmol), base (2.0 mmol), Temp (110 ºC), Time 12 h.

References

[1] W. Hong, J. Wang and E. Wang, *CrystEngComm*, 2015, **17**, 9011.

[2] H.-H. Li, S. Zhao, M. Gong, C.-H. Cui, D. He, H.-W. Liang, L. Wu and S.-H. Yu, *Angew. Chem. Intl. Ed.,* 2013*,* **52**, 7472.